Yokohata *et al.*
Progress in Earth and Planetary Science (2022) 9:39
https://doi.org/10.1186/s40645-022-00498-z

Progress in Earth and Planetary Science

RESEARCH ARTICLE

Open Access

Assessing and projecting surface air temperature conditions required to sustain permafrost in Japan

Tokuta Yokohata[1*], Go Iwahana[2], Kazuyuki Saito[3], Noriko N. Ishizaki[1], Taiga Matsushita[4] and Tetsuo Sueyoshi[3,5]

Abstract

Permafrost covers a wide area of the Northern Hemisphere, including high-altitude mountainous areas and even at mid-latitudes. There is concern that the thawing of mountain permafrost can cause slope instability and substantially impact alpine ecosystems, and because permafrost in mountainous areas is difficult to observe, detailed analyses have not been performed on its current distribution and future changes. Although previous studies have observed permafrost only at a limited number of points in Japan (e.g., Daisetsu Mountains, Mt. Fuji, and Mt. Tateyama in the Northern Japan Alps), we show that permafrost potentially exists in nine domains in Japan (Daisetsu Mountains, Mt. Fuji, Northern and Southern Japan Alps, Hidaka Mountains, Mt. Shiretokodake, Sharidake, Akandake, and Yotei). In the Daisetsu Mountains and Mt. Fuji, the environmental conditions required for maintaining at least some permafrost are projected to remain in the future if a decarbonized society is achieved (RCP2.6 or RCP4.5). However, if greenhouse gas emissions continue to increase (RCP8.5), the environmental conditions required for sustaining permafrost are projected to disappear in the second half of the twenty-first century. In other domains, the environmental conditions required for maintaining permafrost are either projected to disappear in the next ten years (Hidaka Mountains, Northern Japan Alps) or they have almost disappeared already (Southern Japan Alps, Mt. Shiretokodake, Sharidake, Akandake, and Yotei). Our projections show that climate change has a tremendous impact on Japan's mountain permafrost environment and suggests the importance of monitoring the mountain environment and considering measures for adapting to future climate change.

Keywords: Mountain permafrost, Climate change, Future projections

1 Introduction

Areas in which the temperature of the ground falls below 0 °C for two consecutive years are called permafrost (IPCC 2013). Thawing of permafrost in mountains (we call mountain permafrost hereafter) areas has reportedly increased the frequency and scale of rockfalls and landslides (Krautblatter et al. 2013; Lacelle et al., 2015; Patton et al. 2019; Hjort et al. 2022). This threatens the safety of hikers and mountaineers (Purdie et al. 2015) and changes iconic mountaineering routes and suitable climbing seasons (Mourey et al. 2019). In addition, the thawing of mountain permafrost has a substantial impact on alpine ecosystems through changes in temperature, soil moisture and groundwater. The disappearance of mountain permafrost, coupled with inadequate precipitation in summer and reduced snowmelt, can cause a lack of water during the growing season, changes in species composition, and reduced greening and productivity (Trujillo et al. 2012; Sloat et al. 2015). Thawing of mountain permafrost can have a marked impact on mountain ecosystems, including various kinds of alpine plants and

*Correspondence: yokohata@nies.go.jp

[1] Earth System Division, National Institute for Environmental Studies, 16-2, Onogawa, Tsukuba 305-8506, Japan
Full list of author information is available at the end of the article

animals (Jones et al. 2018), which are valuable natural resources that are actively sought out by climbers (Kubo et al. 2018; Mameno et al. 2022).

Studies on future projections of permafrost thawing show that thawing proceeds from the lower latitudes and warmer regions (Yokohata et al. 2020a; Hjort et al. 2022). Therefore, it is considered important to estimate the current and future projected status of permafrost located at the lower latitudinal limits of the permafrost distribution to understand the changes in permafrost due to climate change. According to a study on the global permafrost distribution (Obu et al. 2019; Smith et al. 2022), the lowest-latitude permafrost in the Northern Hemisphere is located in the Himalayas (Iwata et al. 2003; Matsuoka 2002; 2003; Fukui et al. 2007). In Asia, Mt. Fuji (35° N), Mt. Tateyama (37° N), and the Daisetsu Mountains (43° N) in Japan, and the Tianshan Mountains (42° N) and the Daxing Anling Mountains (50° N) in China reportedly contain permafrost (Obu et al. 2019). Among these areas, estimates of the permafrost distribution at the 1 km scale have been compared with observational data for the Tibetan Plateau and mountains in China (Obu et al. 2019). Further, while permafrost in Japan has been reported in the Daisetsu Mountains (Fukuda and Sone 1992; Ishikawa and Hirakawa 2000; Iwahana et al. 2011; Sone and Watanabe 2018; Sone 2020), the lowland of Hokkaido such as Shikaribetsu and Oketo (Sone 1996; Sawada et al. 2003), Mt. Fuji (Higuchi and Fujii 1971; Ikeda et al. 2012), and Mt. Tateyama (Fukui and Iwata 2000; Aoyama 2005) in the Northern Japan Alps, country-scale analyses have not been performed to date.

Future projections of the permafrost distribution have been performed using global climate models (GCMs) (Schneider von Deimling et al. 2015; Chadburn et al. 2017; Gasser et al. 2018; Yokohata et al. 2020b). However, since the general resolution of GCMs is approximately 100 km, it is difficult to estimate the current distribution and to perform future projections of mountain permafrost, which involves more detailed estimates of permafrost at different altitudes (Hock et al. 2019). In a previous study, we used bias-corrected and 1-km downscaled GCM projections (Ishizaki et al. 2020) to estimate the size of areas where climate conditions are suitable for permafrost in Japan's Daisetsu Mountains (Yokohata et al. 2021). In this study, such areas throughout Japan were estimated by employing the methods used in our previous study (Yokohata et al. 2021).

2 Methods

2.1 Bias-corrected and downscaled climate model output

We used the bias-corrected and downscaled climate model outputs developed by Ishizaki et al. (2020) and Ishizaki (2021), who generated two bias-corrected climate scenarios using different methods. We used climate scenarios based on the cumulative distribution function-based downscaling method (CDFDM, developed in previous studies; Iizumi et al. 2010, 2011, 2012). Using the CDFDM, the cumulative distribution function for simulated daily mean data is corrected so that it matches the 1-km resolution meteorological data for Japan (Ohno et al. 2016). Ishizaki et al. (2020) demonstrated that the CDFDM method is superior to other methods, such as Gaussian-type scaling approaches (Haerter et al. 2011). Furthermore, Ishizaki et al. (2020) and Ishizaki (2021) corrected biases in historical simulations and future projections based on the RCP2.6 and RCP8.5 scenarios for four CMIP5 GCMs (i.e., GFDL-CM3; Donner et al. 2011, MIROC5; Watanabe et al. 2010, HadGEM2-ES; Jones et al. 2011, MRI-CGCM3; Yukimoto et al. 2012, Nor-ESM; Bentsen et al. 2013), and the RCP2.6, RCP4.5, and RCP8.5 scenarios for five CMIP6 GCMs (i.e., MIROC6; Tatebe et al. 2019, MRI-ESM2-0; Yukimoto et al. 2019, ACCESS-CM2; Bi et al. 2020, IPSL-CM6A-LR; Boucher et al. 2020, MPI-ESM1-2-HR; Müller et al. 2018) for the Japan region at a resolution of 1 km. Briefly, the reasons why Ishizaki et al. (2020) and Ishizaki (2021) selected nine GCMs from the CMIP5 and CMIP6 GCMs were to account for uncertainties in the ranges of future surface air temperature and precipitation projections with the models and to ensure that they effectively reproduce the twentieth-century climate.

Ishizaki et al. (2020) showed that bias-corrected historical climate scenarios accurately reproduced monthly averaged values; extreme values, such as summer days, and indicators defined by daily values, such as precipitation intensity. In this study, we utilized version 202,005 of CMIP5 (Ishizaki et al. 2020) and version 202,105 of CMIP6 (Ishizaki 2021), in which the time window for the cumulative distribution function (1 month) and the reference period (1980–2018) were modified so that the monthly values corresponded to those for the observations.

2.2 Statistical method for inferring permafrost distribution

The freezing (thawing) index, defined as the cumulative daily temperature below (above) the freezing point of 0 °C, has been used as a proxy for inferring the permafrost distribution. Saito et al. (2014) used this index to develop a high-resolution (2 km) method for estimating the permafrost distribution in northeastern Asia, including the permafrost in Japanese mountainous areas investigated in the present study. We employed the same method to infer the permafrost distribution by using the bias-corrected, 1 km resolution climate scenarios developed by Ishizaki et al. (2020). The

method of Saito et al. (2014) was also used to estimate the permafrost environment for the past 122 kyr (Saito et al. 2022).

Saito et al. (2014) classified the permafrost area in northeastern Asia into two categories based on freezing and thawing indices: (a) climate-driven permafrost (CDP), which are areas where climatic conditions favor the development and/or maintenance of continuous permafrost, and (b) environmentally conditioned permafrost (ECP), which are areas where permafrost development and/or maintenance is dependent upon environmental factors such as ecosystem characteristics, topography or geology. In addition, Saito et al. (2014) divided seasonally frozen ground into two subcategories: (c) ground that undergoes seasonal freezing (SF) and (d) ground that undergoes intermittent freezing (IF). These distinctions were made to distinguish between seasonal frost that is deep and/or persistent and frost that exists for a short time (i.e., < 2 weeks).

Using a freezing index (i.e., the number of days per year when the surface air temperature is below 0 °C multiplied by the surface air temperature), I_f, and the thawing index (i.e., the number of days per year when the surface temperature is above 0 °C multiplied by the surface air temperature), I_t, these permafrost classes can be defined as follows.

(a) CDP

$$I_t < 0.9\, I_f - 2300 \tag{1}$$

(b) ECP

$$0.9 I_f - 2300 < I_t < 2.4 I_f - 3300 \tag{2}$$

(c) SF

$$2.4 I_f - 3300 < I_t \quad \text{and} \quad 30 < I_f \tag{3}$$

(d) IF

$$0 < I_f \leq 30 \tag{4}$$

For consistency with Saito et al. (2014), this study used the monthly mean surface air temperature to calculate the freezing and thawing indices; previous studies have shown that the relative error is less than 5% when using daily or monthly means (Frauenfeld et al. 2007). Saito et al. (2014) performed permafrost classification at a resolution of 2 km by considering the temperature decrease with altitude using spatially detailed elevation data (ETOPO1; Amante and Eakins 2009) that were based on the results of the CMIP5 GCMs. In the present study, a temperature decrease with altitude was considered in the 1-km-mesh observational data (Ohno et al. 2016) that were used for bias-corrected climate scenarios (Ishizaki et al. 2020; Ishizaki 2021).

In this study, the freezing and thawing indices for the past 30 years were averaged to classify the permafrost in each grid cell, similar to Saito et al. (2014). Averaging over 30 years smooths the internal variability in surface air temperature and corresponds to the delayed response of permafrost to climate change.

3 Results and discussion

3.1 Surface air temperature conditions required to sustain permafrost in Japan

Figure 1 (left) shows the altitude distribution of eastern Japan. In general, the annual mean surface air temperature is low at high latitudes and at high altitudes. The correspondence between altitude and the annual mean surface air temperature is shown in Additional file 1: Fig. S1. In eastern Japan, regions with low surface air temperatures are widespread in Hokkaido (the northernmost island of Japan). As shown in Fig. 1a, in Hokkaido, high-altitude mountains exist in the interior (Daisetsu Mountains, 1 in Fig. 1b), southern central region (Hidaka Mountains, 2 in Fig. 1b), and in the east (5, 6 and 8 in Fig. 1b). On the main island of Honshu to the south of Hokkaido, there are particularly high mountains in the central Chubu region (inset at bottom of Fig. 1a), due to the influence of orogeny. In the Chubu region, the high mountainous areas are the Northern Japan Alps (3 in Fig. 1c), the Southern Alps (7 in Fig. 1c), and Mt. Fuji (4 in Fig. 1c).

Figure 1b and c shows an area with climatic conditions that are suitable for permafrost development in the mountainous regions of Japan. These areas are probable locations of permafrost based on nine bias-corrected and downscaled climate scenarios (Ishizaki et al. 2020; Ishizaki 2021) in each grid cell. Permafrost classification in this study is based on Saito et al. (2014), who classified permafrost into CDP and ECP; however, only ECP is present in the mountainous regions of Japan. Given that the actual distribution of permafrost is determined by complex interactions between environmental phenomena, such as topography and geology (Ishikawa and Hirakawa 2000), grid cells that were classified as permafrost in this study indicate only where the climatic conditions are suitable for the maintenance of permafrost. We refer to areas containing these grid cells as an "ECP region". In addition to surface air temperature, snow cover is an important factor affecting the distribution of permafrost (Ishikawa and Hirakawa 2000). In general, permafrost is distributed in wind-blown gravel areas where the snow cover is typically thin. Furthermore, it has been noted that mountain permafrost distribution is greatly limited by thawing of frozen soil due to the percolation of

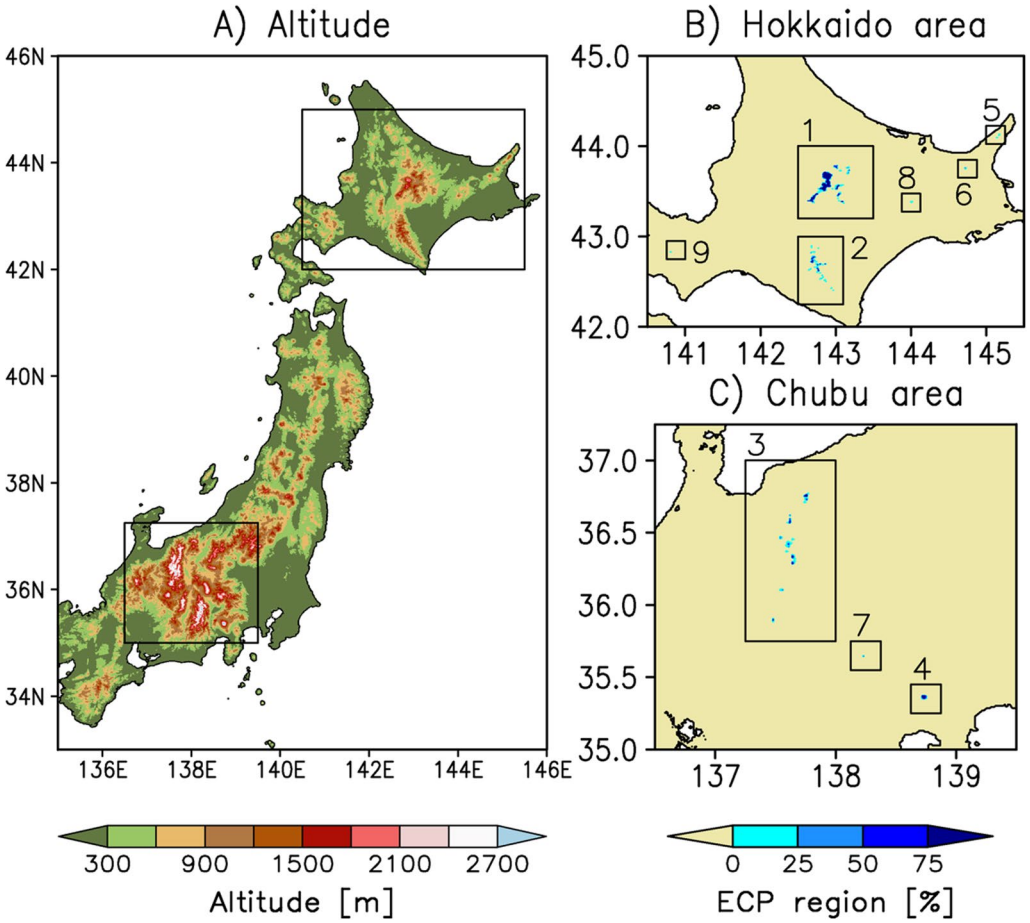

Fig. 1 **a** Map showing the altitude [m] of northern and eastern Japan, and the distribution of regions with surface air temperatures that favor the maintenance of permafrost (the Environmentally Conditioned Permafrost regions) in Japan; **b** Hokkaido and **c** the Chubu. The numbers indicate (1) Daisetsu Mountains, (2) Hidaka Mountains, (3) Northern Japan Alps, (4) Mt. Fuji, (5) Mt. Shiretokodake, (6) Mt. Shari, (7) Southern Japan Alps, (8) Mt. Akandake, and (9) Mt. Yotei. The distribution of the environmentally conditioned permafrost region is based on probabilities estimated by nine bias-corrected climate scenarios

rainfall during the summer (Fukui 2003, 2004; Ikeda and Iwahana 2010, Ikeda et al. 2012). Due to the limited distribution of wind-blown gravel areas and the percolation of rainfall, the actual distribution of permafrost would be smaller than the area estimated using only surface air temperatures.

The ECP regions estimated in this study under current climate conditions, in descending order of area, are (1) the Daisetsu Mountains, (2) the Hidaka Mountains, (3) the Northern Japan Alps, (4) Mt. Fuji, (5) Mt. Shiretokodake, (6) Mt. Sharidake, (7) the Southern Japan Alps, (8) Mt. Akandake, and (9) Mt. Yotei. In general, ECP regions are located in high-latitude and high-altitude mountainous regions where the surface air temperature is low throughout the year.

Figure 2 shows the details of the ECP regions in the nine areas. Regions identified as ECP regions with high confidence in multi-model estimations (i.e., large value in Fig. 2) are (1) the Daisetsu Mountains, (2) the Hidaka Mountains, (3) the Northern Japan Alps, and (4) Mt. Fuji. In Fig. 2, the points where permafrost was confirmed by previous observational studies are shown in red (the details of the observational sites are shown in Additional file 1: Table S1). The permafrost observations in previous studies (Higuchi and Fujii 1971; Fukuda and Sone 1992; Ishikawa and Hirakawa 2000; Fukui and Iwata 2000; Aoyama 2005; Iwahana et al. 2011; Ikeda et al. 2012; Sone and Watanabe 2018; Sone 2020) are consistent with the findings of the present study, as shown in Fig. 2. The ECP region exists at altitudes higher than 1600 m in the Daisetsu and Hidaka Mountains in Hokkaido. Permafrost has not been observed in the Hidaka Mountains to date, but our results indicate that permafrost could exist at altitudes higher than 1600 m in the Hidaka Mountains.

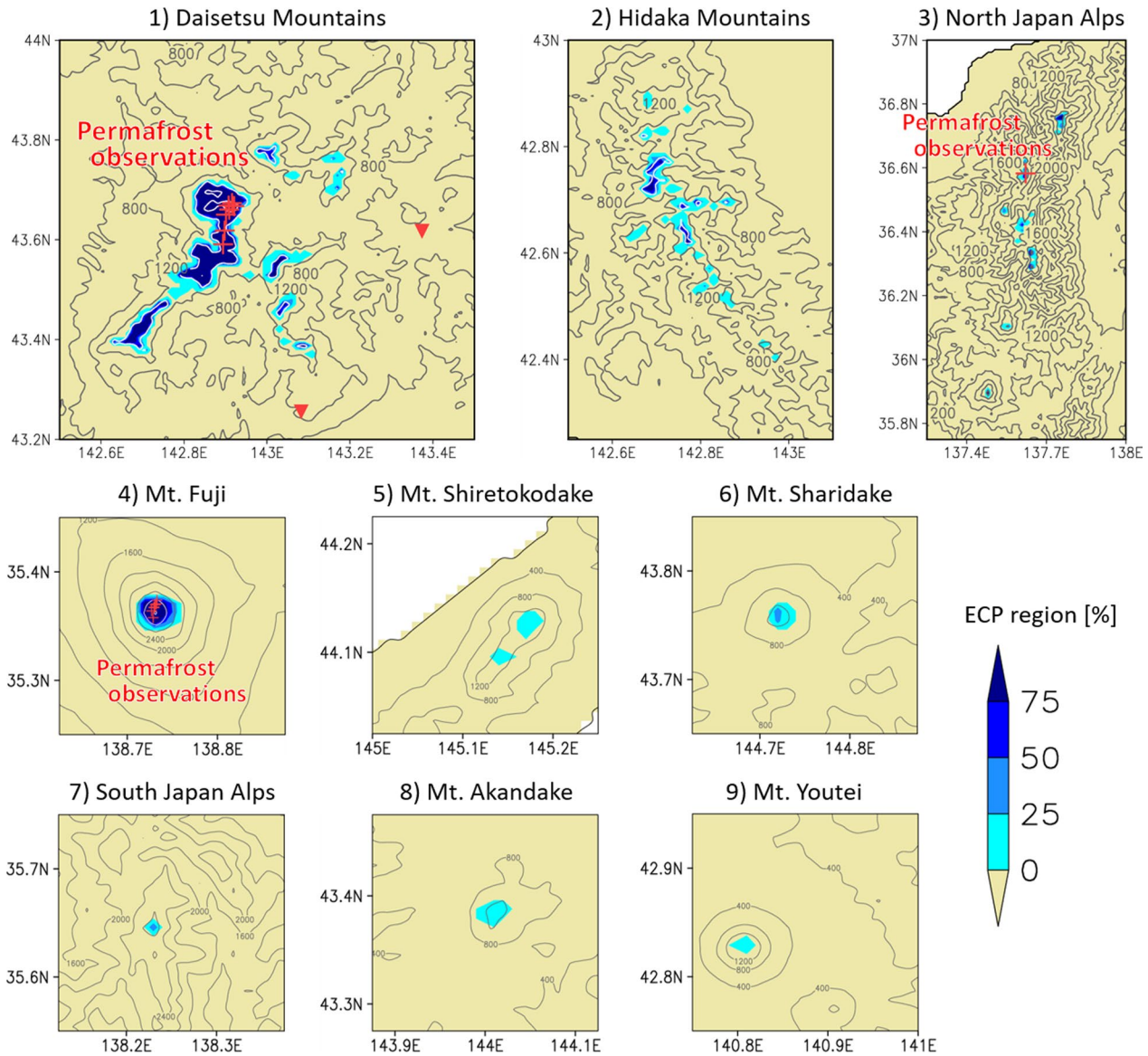

Fig. 2 Distribution of regions with surface air temperatures that favor the maintenance of permafrost (the Environmentally Conditioned Permafrost regions) in Japan under the current climate conditions (averaged over 1999–2018); (1) Daisetsu Mountains, (2) Hidaka Mountains, (3) Northern Japan Alps, (4) Mt. Fuji, (5) Mt. Shiretokodake, (6) Mt. Sharidake, (7) Southern Japan Alps, (8) Mt. Akandake, and (9) Mt. Yotei. The distribution of the environmentally conditioned permafrost region is based on probabilities estimated by nine bias-corrected climate scenarios. Red points indicate sites where permafrost has been observed. The observations of sporadic permafrost in Shikaribetsu and Oketo are shown as ▼, and other observations are shown as +. See Additional file 1: Table S1 for details. The contour interval is 400 m

Permafrost has been observed at Tateyama in the Northern Japan Alps (Fukui and Iwata 2000; Aoyama 2005), but could exist on other mountains at altitudes above 2600 m. Mt. Fuji is located at a lower latitude than other areas, but the area above 3000 m is identified as an ECP region, which is consistent with previous studies (Ikeda et al. 2012). We also confirmed that the annual mean surface air temperature at the field observation sites in these mountains is consistent with the observational data, as shown in Additional file 1: Fig. S2.

It should be noted that sporadic permafrost has been observed in the lower altitudes of the mountain flanks (shown as ▼ in Fig. 2-1 at Shikaribetsu and Oketo with an altitude of 1254 m and 480 m, respectively), which formed under exceptionally cold conditions at the specific geomorphological locations of Fuketsu, or wind

caves (Sone 1996; Sawada et al. 2003). Our analysis is based on spatially averaged surface air temperatures on the 1-km scale and thus does not represent permafrost in such extraordinary conditions defined as extra-zonal permafrost (Ishikawa et al. 2003).

Regions with low confidence in projections from multiple bias-corrected and downscaled GCMs are (5) Mt. Shiretokodake, (6) Mt. Sharidake, (7) the Southern Japan Alps, (8) Mt. Akandake, and (9) Mt. Yotei (Fig. 2). In these domains, ECP regions exist at altitudes above 1400 m (Mt. Shiretokodake), 1200 m (Mt. Sharidake), 3000 m (Southern Japan Alps), 1300 m (Mt. Akandake), and 1800 m (Mt. Yotei).

Since latitude and altitude are important geographical factors that determine the surface air temperature, they also affect the distribution of permafrost. Figure 3 shows a scatterplot of the latitude–altitude distribution in the ECP regions under present climate conditions. We use the grid mean altitudes (Ohno et al. 2016) for the scatter plot. In Fig. 3, the regression line is calculated by selecting points corresponding to the lowest altitude at each latitude. Thus, the lower altitude limit for the ECP region in mountainous regions of Japan in the present climate is given by:

$$\text{Altitude} = 2997 - (\text{latitude} - 35) \times 177 \text{ [m]} \quad (5)$$

The lower altitude limit, which is approximately 2997 m at a latitude of 35° N, decreases by 177 m as the latitude increases by 1°. This is consistent with the latitudinal variation of the lower limit of mountain permafrost in Asia has a north–south tilt of 160 m per degree (Matsuoka 2002; 2003).

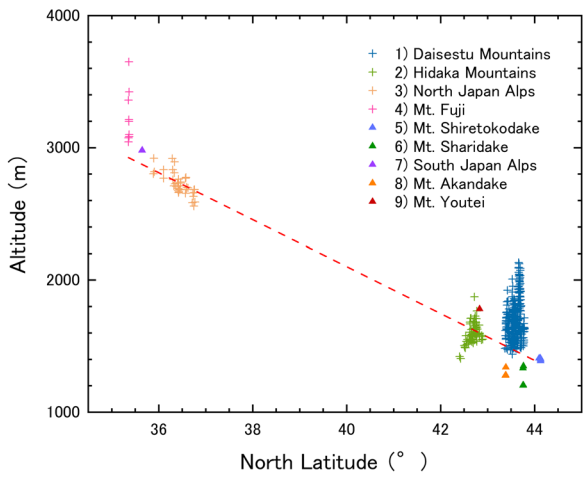

Fig. 3 Latitude–altitude distribution of surface air temperature that maintains permafrost. The colors or shapes of symbols differ for each of the nine regions shown in Fig. 1. The red regression line is calculated using the points that take the lowest altitude at each latitude

3.2 Projecting surface air temperature conditions required to sustain permafrost in Japan

Figure 4 shows a time series of changes in the area of ECP regions in Japan. As in Fig. 2, it shows the results for nine domains beginning with the largest ECP region under the current climate conditions. Based on the time series of future projections, the ECP regions in Japan can be classified into the following three types: (a) long-term sustained: Daisetsu Mountains and Mt. Fuji, (b) Borderline: Hidaka Mountains and Northern Japan Alps, and (c) In crisis: other domains.

3.2.1 Long-term sustained: Daisetsu Mountains and Mt. Fuji

For the Daisetsu Mountains and Mt. Fuji, the ECP regions are projected to be sustainable over the long term. This is because there is a large difference between the mountaintop altitude and the lower limit altitude of the ECP region under the current climate (Fig. 3). As the surface air temperature rises in the future, the altitude of the lower part of the ECP region will also rise. However, for the Daisetsu Mountains and Mt. Fuji, the time at which the lower altitude limit for the ECP region is projected to reach the mountain summit (i.e., when the ECP regions will disappear) depends on the climate scenario.

Currently, the Daisetsu Mountains have the largest ECP region in Japan; however, the spatial extent of this ECP region is estimated to have decreased since around 2000, and it is projected that the ECP regions will disappear around 2070, regardless of the model used, under the RCP8.5 scenario (Fig. 4). On the other hand, under the RCP2.6 scenario, which stabilizes the future global mean surface air temperature rise to about 2 °C, the ensemble average of the ECP regions is projected to remain at approximately 20 km^2 by 2100. Under the RCP4.5 scenario, the ensemble average of the ECP regions is projected to remain at approximately 10 km^2. The results of RCP8.5 and 2.6 scenarios in the present study are consistent with Yokohata et al. (2021), which used only four GCMs for the future projection, while those of RCP4.5 were not included in Yokohata et al. (2021).

Due to the low latitude of Mt. Fuji (approximately 35° N), its ECP regions are relatively small (approximately 8 km^2 in total based on the 2010 ensemble average). However, due to its high altitude, the ECP region is projected to persist long into the future. Under the RCP8.5 scenario, the ECP regions on Mt. Fuji are projected to disappear at around 2100 based on the ensemble average. The ECP regions are projected to be sustained at approximately 2 km^2 under RCP2.6 and approximately 1 km^2 under RCP4.5.

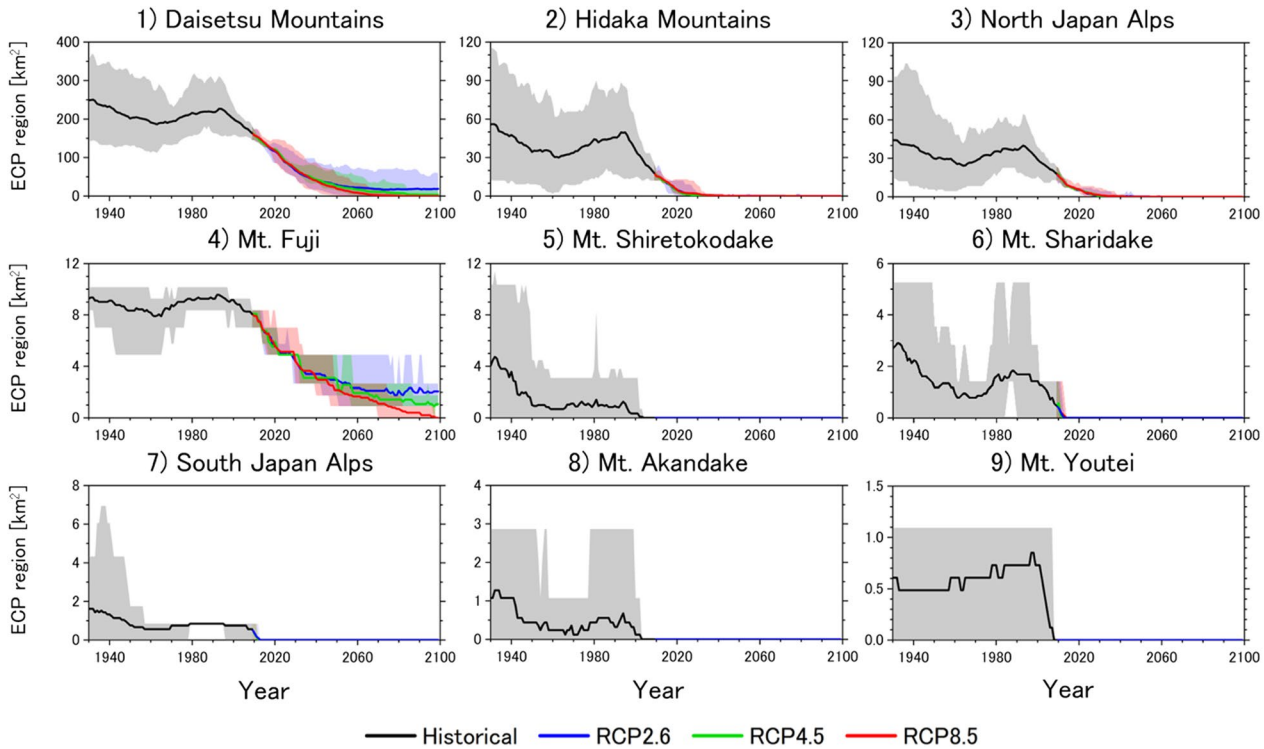

Fig. 4 Time sequence of areas in mountainous regions of Japan with surface air temperatures that favor the maintenance of permafrost; (1) Daisetsu Mountains, (2) Hidaka Mountains, (3) Northern Japan Alps, (4) Mt. Fuji, (5) Mt. Shiretokodake, (6) Mt. Shari, (7) Southern Japan Alps, (8) Mt. Akandake, (9) Mt. Yotei. Historical simulations (black) and future projections for the RCP2.6 (blue), RCP4.5 (green), and RCP8.5 (red) scenarios are shown. Shading indicates the minima and maxima of multi-model projections, and the thick line indicates the multi-model average

3.2.2 Borderline: Hidaka Mountains and Northern Japan Alps

The Hidaka Mountains and the Northern Alps are domains where ECP regions are currently thought to exist, but which are likely to disappear by 2030 regardless of the climate scenario (Fig. 4). This is because the lower altitude limit of the ECP region in the current climate is relatively close to the altitude of the mountain summit. In the Hidaka Mountains and the Northern Alps, the ECP regions are currently projected to be several tens of square kilometers, and it is estimated that they will disappear in the next 10 years. It is projected that the ECP regions in the Hidaka Mountains and Northern Japan Alps will be lost due to the rapid increase in surface temperature in the high-latitude regions, which has been occurring since the 2000s (Fig. 7 in Yokohata et al. 2021).

3.2.3 In crisis: other domains

In the five domains with low concordance with multi-model projections for ECP regions under the current climate (< 20%), including Mt. Shiretokodake, Mt. Shari, the Southern Japan Alps, Mt. Akan, and Mt. Yotei, the ECP regions are estimated to decrease rapidly beginning in the 2000s (Fig. 4) and are projected to disappear before 2020. In these domains, the mountaintop altitudes are even lower and the areas of the ECP region are smaller than those for the Hidaka Mountains and the Northern Alps (approximately several km^2), and thus, the rate of disappearance is projected to be even faster than those in these latter two domains.

4 Conclusions

The analysis in this study clarified, for the first time, the distribution of the temperature environment that sustains permafrost in mountainous areas throughout Japan. Due to the difficulties associated with in situ observations of permafrost in mountainous areas, the existence of mountain permafrost has only been reported in a limited number of places, such as in the Daisetsu Mountains, Mt. Fuji, and Mt. Tateyama in the Northern Japan Alps of Japan (Higuchi and Fujii 1971; Fukuda and Sone 1992; Ishikawa and Hirakawa 2000; Fukui and Iwata 2000; Aoyama 2005; Iwahana et al. 2011; Ikeda et al. 2012; Sone and Watanabe 2018; Sone 2020). However, the findings of this study show that permafrost could exist in other regions, such as the Hidaka Mountains, Mt. Shiretokodake, Mt. Sharidake, the Southern Japan Alps, Mt. Akandake and Mt. Yotei (Fig. 2). Our results will therefore aid in the

selection of candidate sites for mountain permafrost observations in Japan.

Furthermore, for the first time, we performed projections of environmental conditions to identify mountainous areas that are well suited to sustaining permafrost throughout Japan and showed that changes in the possible distribution of permafrost can vary greatly among regions. At present, the domain with the largest ECP region is the Daisetsu Mountains in Hokkaido, where the latitude and altitude are both high and the annual average temperature is low. Predictions for the future ECP area of Daisetsuzan will differ depending on the climate scenario that is applied. Under RCP8.5, where greenhouse gas concentrations continue to increase, the ECP region will disappear in the second half of the twenty-first century. However, under the RCP2.6 or the RCP4.5 scenarios, where the future global mean surface air temperature change is stabilized at 2 °C and < 3 °C, respectively, the ECP regions are projected to remain at approximately 20 km^2 and 10 km^2, respectively. Similarly, at Mt. Fuji, which has a low latitude but a high altitude, the ECP regions are projected to disappear around 2100 under the RCP8.5 scenario. However, if the RCP2.6 or RCP4.5 scenarios are realized, the ECP regions at Mt. Fuji are projected to remain at approximately 2 km^2 or 1 km^2, respectively. Successful attempts to stabilize the climate in the twenty-first century may leave a small area capable of sustaining permafrost.

Although ECP regions are projected to persist in the Daisetsu Mountains and Mt. Fuji after the latter half of the twenty-first century, the risk of disappearance is higher for the ECP regions in other domains. In the Hidaka Mountains and the Northern Japan Alps, where the latitude and mountaintop altitude are relatively high, the ECP regions are projected to disappear in the next ten years or so, irrespective of the climate scenario. In the other five domains, Mt. Shiretokodake, Mt. Sharidake, Southern Japan Alps, Mt. Akandake, and Mt. Yotei, most of the ECP regions are also projected to disappear shortly. Indeed, the mode of seasonal freezing in these domains may already have changed significantly.

The analysis presented in this study does not consider detailed factors such as topography (slope direction and slope angle), soil properties (porosity and permeability), vegetation, and meteorological conditions (precipitation, local wind direction and snow cover), which are known to play important roles in determining the distribution of permafrost (e.g., Ishikawa and Hirakawa 2000). Using a 30-year average as the calculation period for the freezing and thawing indices, hysteresis in surface air temperature changes is considered in our estimates for the ECP region (see Methods). However, the response of permafrost to changes in climatic conditions may occur over a much longer timescale (Saito et al. 2014), and changes in permafrost distributions may be slower than those shown in Fig. 4.

The climatic conditions under which permafrost can exist in Japan's mountainous regions are expected to disappear, indicating the importance of monitoring the environment and developing adaptation measures for climate change. Specifically, monitoring the phenology and distribution of alpine vegetation is considered important for clarifying the effects of permafrost thawing on alpine ecosystems (Yokohata et al. 2021). Accurately monitoring environmental changes in mountainous areas is also vital for addressing the problem of increases in the scale and frequency of flow slopes and landslides (Krautblatter et al. 2013; Lacelle et al. 2015; Patton et al. 2019). Thus, applying a technique to determine the ground-surface displacement in detail by using satellite data is considered necessary (Iwahana et al. 2016; Abe et al. 2020). In addition to accurately monitoring changes in mountain environments, providing local governments with appropriate measures to prepare for major future environmental changes is an essential issue for future studies.

Abbreviations

CDP: Climate-driven permafrost; ECP: Environmentally conditioned permafrost; IF: Intermittent freezing; SF: Seasonal freezing.

Supplementary Information

The online version contains supplementary material available at https://doi.org/10.1186/s40645-022-00498-z.

Additional file 1, Information for locations of permafrost occurrence based on observations (**Table S1**), distribution of altitude and annual mean surface air temperature in Japan (**Figure S1**), and time series of annual mean surface air temperatures at the locations where we detected environmentally conditioned permafrost regions (**Figure S2**).

Acknowledgements

We thank Masao Uchida, Yusuke Satoh for their assistance with field observations in the Daisetsu Mountains. We also thank FORTE Science Communications for proofreading the English used in this manuscript.

Author contributions

T.Y. and K.S. proposed the topic and conceived and designed the study. G.I. provided permafrost observation data. N.N.I. contributed to preparing the bias-corrected and downscaled climate model outputs. T.M. contributed to data analysis and drawing figures. All authors discussed and commented on the outcomes. All authors have read and approved the final manuscript.

Funding

This work is supported by TOUGOU, an "Integrated Research Program for Advancing Climate Models" administered by the Ministry of Education, Culture, Sports, Science and Technology of Japan (Grant Number JPMXD0717935715). Acquisition of permafrost observation data was supported by JSPS KAKENHI (18H03353). This work was supported in part by the Arctic Challenge for Sustainability II (ArCS II) (Program Grant Number JPMXD1420318865). This work was also supported in part by the Climate Change Adaptation and Decarbonized and Sustainable Society Research Program at the National Institute for Environmental Studies.

Availability of data and materials

Data sharing is not applicable to this article as no datasets were generated or analyzed during the current study. Please contact the author for data requests. The bias-corrected meteorological dataset is available at https://www.nies.go.jp/doi/10.17595/20210501.001-e.html.

Declarations

Competing interests

The authors declare that they have no competing interests.

Author details

[1]Earth System Division, National Institute for Environmental Studies, 16-2, Onogawa, Tsukuba 305-8506, Japan. [2]International Arctic Research Center, University of Alaska Fairbanks, Fairbanks, USA. [3]Research Institute for Global Change, Japan Agency for Marine-Earth Science and Technology, Yokohama, Japan. [4]Faculty of Life and Environmental Sciences, University of Tsukuba, Tsukuba, Japan. [5]International Affairs and Research Development Office, National Institute of Polar Research, Tokyo, Japan.

Received: 15 April 2022 Accepted: 29 June 2022
Published online: 02 August 2022

References

Abe T, Iwahana G, Efremov PV, Desyatkin AR, Kawamura T, Fedorov A, Zhegusov Y, Yanagiya K, Tadono T (2020) Surface displacement revealed by L-band InSAR analysis in the Mayya area, Central Yakutia, underlain by continuous permafrost. Earth Planets Space 72:138

Amante C, Eakins BW (2009) ETOPO1 1 arc-minute global relief model: procedures, data sources and analysis. NOAA Technical Memorandum NESDIS NGDC-24

Aoyama M (2005) Rock glaciers in the northern Japanese Alps: palaeoenvironmental implications since the Late Glacial. J Quat Sci 20:471–484

Bentsen M, Bethke I, Debernard JB, Iversen T, Kirkevåg A, Seland Ø, Drange H, Roelandt C, Seierstad IA, Hoose C, Kristjánsson JE (2013) The Norwegian earth system model, NorESM1-M—Part 1: description and basic evaluation of the physical climate. Geosci Model Dev 6:687–720

Bi D, Dix M, Marsland S, O'Farrell S, Sullivan A, Bodman R, Law R, Harman I, Srbinovsky J, Rashid HA, Dobrohotoff P, Mackallah C, Yan H, Hirst A, Savita A, Dias FB, Woodhouse M, Fiedler R, Heerdegen A (2020) Configuration and spin-up of ACCESS-CM2, the new generation Australian community climate and earth system simulator coupled model. J South Hemisph Earth Syst Sci 70:225–251

Boucher O, Servonnat J, Albright AL, Aumont O, Balkanski Y, Bastrikov V, Bekki S, Bonnet R, Bony S, Bopp L, Braconnot P, Brockmann P, Cadule P, Caubel A, Cheruy F, Codron F, Cozic A, Cugnet D, D'Andrea F, Davini P, de Lavergne C, Denvil S, Deshayes J, Devilliers M, Ducharne A, Dufresne J-L, Dupont E, Éthé C, Fairhead L, Falletti L et al (2020) Presentation and evaluation of the IPSL-CM6A-LR climate model. J Adv Model Earth Syst 12:e2019MS002010

Chadburn SE, Burke EJ, Cox PM, Friedlingstein P, Hugelius G, Westermann S (2017) An observation-based constraint on permafrost loss as a function of global warming. Nat Clim Change 7:340–344

Donner LJ, Wyman BL, Hemler RS, Horowitz LW, Ming Y, Zhao M, Golaz J-C, Ginoux P, Lin SJ, Schwarzkopf MD, Austin J, Alaka G, Cooke WF, Delworth TL, Freidenreich SM, Gordon CT, Griffies SM, Held IM, Hurlin WJ, Klein SA, Knutson TR, Langenhorst AR, Lee H-C, Lin Y, Magi BI, Malyshev SL, Milly PCD, Naik V, Nath MJ, Pincus R et al (2011) The dynamical core, physical parameterizations, and basic simulation characteristics of the atmospheric component AM3 of the GFDL global coupled model CM3. J Clim 24:3484–3519

Frauenfeld OW, Zhang T, Mccreight JL (2007) Northern hemisphere freezing/thawing index variations over the twentieth century. Int J Climatol 27:47–63

Fukuda M, Sone T (1992) Some characteristics of alpine permafrost, Mt. Daisetsu, Central Hokkaido, Northern Japan. Geogr Ann Ser B 74:159–167. https://doi.org/10.1080/04353676.1992.11880359

Fukui K, Iwata S (2000) Result of permafrost investigation in Kuranosuke Cirque, Tateyama, the Japanese Alps. J Jpn Soc Snow Ice 62:23–28 (**(in Japanese with English abstract)**)

Fukui K (2003) Investigating mountain permafrost distribution by ground temperature measurements in the Tateyama Mountains, the northern Japanese Alps, central Japan. Z Geomorphol Neue Folge Suppl 130:179–193

Fukui K (2004) Formation and preservation processes of mountain permafrost in Tateyama Mountains, the northern Japanese Alps, central Japan. J Jpn Soc Snow Ice 66:187–195 (**(in Japanese with English abstract)**)

Fukui K, Fujii Y, Ageta Y, Asahi K (2007) Changes in the lower limit of mountain permafrost between 1973 and 2004 in the Khumbu Himal, the Nepal Himalayas. Glob Planet Change 55:251–256

Gasser T, Kechiar M, Ciais P, Burke EJ, Kleinen T, Zhu D, Huang Y, Ekici A, Obersteiner M (2018) Path-dependent reductions in CO_2 emission budgets caused by permafrost carbon release. Nat Geosci 11:830–835

Haerter JO, Hagemann S, Moseley C, Piani C (2011) Climate model bias correction and the role of timescales. Hydrol Earth Syst Sci 15:1065–1079

Higuchi K, Fujii Y (1971) Permafrost at the summit of Mount Fuji, Japan. Nature 230:521–521

Hjort J, Streletskiy D, Doré G, Wu Q, Bjella K, Luoto M (2022) Impacts of permafrost degradation on infrastructure. Nat Rev Earth Environ 3:24–38

Hock R, Rasul G, Adler C, Cáceres B, Gruber S, Hirabayashi S, Jackson M, Kääb A, Kang S, Kutuzov S, Milner A, Molau U, Morin S, Orlove B, Steltzer H (2019) High mountain areas. In: Pörtner HO, Roberts DC, Masson-Delmotte V, Zhai P, Tignor M, Poloczanska E, Mintenbeck K, Alegría A, Nicolai M, Okem A, Petzold J, Rama B, Weyer NM (eds) IPCC special report on the ocean and cryosphere in a changing climate

Iizumi T, Nishimori M, Dairaku K, Adachi SA, Yokozawa M (2011) Evaluation and intercomparison of downscaled daily precipitation indices over Japan in present-day climate: Strengths and weaknesses of dynamical and bias correction-type statistical downscaling methods. J Geophys Res Atmos 116:D01111

Iizumi T, Takayabu I, Dairaku K, Kusaka H, Nishimori M, Sakurai G, Ishizaki NN, Adachi SA, Semenov MA (2012) Future change of daily precipitation indices in Japan: a stochastic weather generator-based bootstrap approach to provide probabilistic climate information. J Geophys Res Atmos 117:D11114

Iizumi T, Yokozawa M, Nishimori M (2010) Probabilistic evaluation of climate change impacts on paddy rice productivity in Japan. Clim Change 107:391–415

Ikeda A, Iwahana G (2010) Thawing processes of frozen ground on the summit of Mt Fuji; a preliminary assessment of long-term variations of permafrost. J Geogr 119:917–923 (**(in Japanese with English abstract)**)

Ikeda A, Iwahana G, Sueyoshi T (2012) Year-round monitoring of shallow ground temperatures at high altitudes of Mt. Fuji with a critical discussion on the popular belief of rapid permafrost degradation. J Geogr 121:306–331 (**(in Japanese with English abstract)**)

IPCC (2013) Annex III: Glossary [Planton, S. (ed.)]. In: Stocker TF, Qin D, Plattner G-K, Tignor M, Allen SK, Boschung J, Nauels A, Xia Y, Bex V, Midgley PM (eds) Climate Change 2013: the physical science basis. Contribution of Working Group I to the Fifth Assessment Report of the Intergovernmental Panel on Climate Change. Cambridge University Press, Cambridge, United Kingdom and New York, NY, USA.

Ishikawa M, Hirakawa K (2000) Mountain permafrost distribution based on BTS measurements and DC resistivity soundings in the Daisetsu Mountains, Hokkaido, Japan. Permafrost Periglac Process 11:109–123

Ishikawa M, Fukui K, Aoyama M, Ikeda A, Sawada Y, Matsuoka N (2003) Mountain permafrost in Japan: distribution, landforms and thermal regimes. Z Geomorphol Neue Folge Suppl 130:99–116

Ishizaki NN, Nishimori M, Iizumi T, Shiogama H, Hanasaki N, Takahashi K (2020) Evaluation of two bias-correction methods for gridded climate scenarios over Japan. SOLA 16:80–85

Ishizaki NN (2021) Bias corrected climate scenarios over Japan based on CDFDM method using CMIP6. https://doi.org/10.17595/20210501.001

Iwahana G, Sawada Y, Katamura F, Ishikawa M, Sone T, Sueyoshi T, Harada K (2011) Monitoring of permafrost in the Daisetsu mountains 2005–2010, JSSI & JSSE Joint Conference, Nagaoka, Niigata, https://doi.org/10.14851/jcsir.2011.0.88.0 (in Japanese)

Iwahana G, Harada K, Uchida M, Tsuyuzaki S, Saito K, Narita K, Kushida K, Hinzman LD (2016) Geomorphological and geochemistry changes in

permafrost after the 2002 tundra wildfire in Kougarok, Seward Peninsula, Alaska. J Geophys Res Earth Surf 121:1697–1715
Iwata S, Naito N, Narama C (2003) Rock glaciers and the lower limit of mountain permafrost in the Bhutan Himalayas. Z Geomorphol Neue Folge Suppl 130:129–143
Jones CD, Hughes JK, Bellouin N, Hardiman SC, Jones GS, Knight J, Liddicoat S, O'Connor FM, Andres RJ, Bell C, Boo KO, Bozzo A, Butchart N, Cadule P, Corbin KD, Doutriaux-Boucher M, Friedlingstein P, Gornall J, Gray L, Halloran PR, Hurtt G, Ingram WJ, Lamarque JF, Law RM, Meinshausen M, Osprey S, Palin EJ, Parsons Chini L, Raddatz T, Sanderson MG et al (2011) The HadGEM2-ES implementation of CMIP5 centennial simulations. Geosci Model Dev 4:543–570
Jones DB, Harrison S, Anderson K, Betts RA (2018) Mountain rock glaciers contain globally significant water stores. Sci Rep 8:2834
Krautblatter M, Funk D, Günzel FK (2013) Why permafrost rocks become unstable: a rock–ice-mechanical model in time and space. Earth Surf Proc Land 38:876–887
Kubo T, Shoji Y, Tsuge T, Kuriyama K (2018) Voluntary contributions to hiking trail maintenance: evidence from a field experiment in a National Park, Japan. Ecol Econ 144:124–128
Lacelle D, Brooker A, Fraser RH, Kokelj SV (2015) Distribution and growth of thaw slumps in the Richardson mountains-peel plateau region, Northwestern Canada. Geomorphology 235:40–51
Mameno K, Kubo T, Oguma H, Amagai Y, Shoji Y (2022) Decline in the alpine landscape aesthetic value in a national park under climate change. Clim Change 170:35
Matsuoka N (2002) Mountain permafrost and periglacial environment in Asia. J Geogr 111:531–545 (**(in Japanese with English abstract)**)
Matsuoka N (2003) Contemporary permafrost and periglaciation in Asian high mountains: an overview. Z Geomorphol Neue Folge Suppl 130:145–166
Mourey J, Marcuzzi M, Ravanel L, Pallandre F (2019) Effects of climate change on high Alpine mountain environments: evolution of mountaineering routes in the Mont Blanc massif (Western Alps) over half a century. Arct Antarct Alp Res 51:176–189
Müller WA, Jungclaus JH, Mauritsen T, Baehr J, Bittner M, Budich R, Bunzel F, Esch M, Ghosh R, Haak H, Ilyina T, Kleine T, Kornblueh L, Li H, Modali K, Notz D, Pohlmann H, Roeckner E, Stemmler I, Tian F, Marotzke J (2018) A higher-resolution version of the Max Planck Institute Earth System Model (MPI-ESM1.2-HR). J Adv Model Earth Syst 10:1383–1413
Obu J, Westermann S, Bartsch A, Berdnikov N, Christiansen HH, Dashtseren A, Delaloye R, Elberling B, Etzelmüller B, Kholodov A, Khomutov A, Kääb A, Leibman MO, Lewkowicz AG, Panda SK, Romanovsky V, Way RG, Westergaard-Nielsen A, Wu T, Yamkhin J, Zou D (2019) Northern hemisphere permafrost map based on TTOP modelling for 2000–2016 at 1 km^2 scale. Earth Sci Rev 193:299–316
Ohno H, Sasaki K, Ohara G, Nakazono KOU (2016) Development of grid square air temperature and precipitation data compiled from observed, forecasted, and climatic normal data. Clim Biosphere 16:71–79 (**(in Japanese with English abstract)**)
Patton AI, Rathburn SL, Capps DM (2019) Landslide response to climate change in permafrost regions. Geomorphology 340:116–128
Purdie H, Gomez C, Espiner S (2015) Glacier recession and the changing rockfall hazard: implications for glacier tourism. NZ Geogr 71:189–202
Saito K, Marchenko S, Romanovsky V, Hendricks A, Bigelow N, Yoshikawa K, Walsh J (2014) Evaluation of LPM permafrost distribution in NE Asia reconstructed and downscaled from GCM simulations. Boreas 43:733–749
Saito K, Ji O, Machiya H, Iwahana G, Ohno H, Yokohata T (2022) Climatic assessment of circum-Arctic permafrost zonation over the last 122 kyr. Polar Sci 31:100765
Sawada Y, Ishikawa M, Ono Y (2003) Thermal regime of sporadic permafrost in a block slope on Mt. Nishi-Nupukaushinupuri, Hokkaido Island, Northern Japan. Geomorphology 52:121–130
Schneider von Deimling T, Grosse G, Strauss J, Schirrmeister L, Morgenstern A, Schaphoff S, Meinshausen M, Boike J (2015) Observation-based modelling of permafrost carbon fluxes with accounting for deep carbon deposits and thermokarst activity. Biogeosciences 12:3469–3488
Sloat LL, Henderson AN, Lamanna C, Enquist BJ (2015) The effect of the Foresummer drought on carbon exchange in subalpine meadows. Ecosystems 18:533–545
Smith SL, O'Neill HB, Isaksen K, Noetzli J, Romanovsky VE (2022) The changing thermal state of permafrost. Nat Rev Earth Environ 3:10–23
Sone T (1996) Degradation of extra-zonal permafrost near Kanoko Dam, Oketo town, Hokkaido, Northern Japan. Q J Geogr 48:293–302 (**(in Japanese with English abstract)**)
Sone T (2020) Ground surface temperatures on the windward bare ground in the Daisetsu Mountains. In: Summaries of JSSI and JSSE Joint Conference on Snow and Ice Research—2020 online, Session ID A2–5. https://doi.org/10.14851/jcsir.2020.0_19 (in Japanese)
Sone T, Watanabe T (2018) Lower limit of permafrost distribution on the windbeaten bare ground in the Daisetsu Mountains, Hokkaido Proceedings of the General Meeting of the Association of Japanese Geographers, No. 93, p 87. https://doi.org/10.14866/ajg.2018s.0_000320 (in Japanese with English abstract)
Tatebe H, Ogura T, Nitta T, Komuro Y, Ogochi K, Takemura T, Sudo K, Sekiguchi M, Abe M, Saito F, Chikira M, Watanabe S, Mori M, Hirota N, Kawatani Y, Mochizuki T, Yoshimura K, Takata K, O'Ishi R, Yamazaki D, Suzuki T, Kurogi M, Kataoka T, Watanabe M, Kimoto M (2019) Description and basic evaluation of simulated mean state, internal variability, and climate sensitivity in MIROC6. Geosci Model Dev 12:2727–2765
Trujillo E, Molotch NP, Goulden ML, Kelly AE, Bales RC (2012) Elevation-dependent influence of snow accumulation on forest greening. Nat Geosci 5:705–709
Watanabe M, Suzuki T, O'ishi R, Komuro Y, Watanabe S, Emori S, Takemura T, Chikira M, Ogura T, Sekiguchi M, Takata K, Yamazaki D, Yokohata T, Nozawa T, Hasumi H, Tatebe H, Kimoto M, (2010) Improved climate simulation by MIROC5: mean states, variability, and climate sensitivity. J Clim 23:6312–6335
Yokohata T, Saito K, Ito A, Ohno H, Tanaka K, Hajima T, Iwahana G (2020a) Future projection of greenhouse gas emissions due to permafrost degradation using a simple numerical scheme with a global land surface model. Prog Earth Planet Sci 7:56
Yokohata T, Saito K, Takata K, Nitta T, Satoh Y, Hajima T, Sueyoshi T, Iwahana G (2020b) Model improvement and future projection of permafrost processes in a global land surface model. Prog Earth Planet Sci 7:69
Yokohata T, Iwahana G, Sone T, Saito K, Ishizaki NN, Kubo T, Oguma H, Uchida M (2021) Projections of surface air temperature required to sustain permafrost and importance of adaptation to climate change in the Daisetsu mountains. Jpn Sci Reports 11:15518
Yukimoto S, Adachi Y, Hosaka M, Sakami T, Yoshimura H, Hirabara M, Tanaka TY, Shindo E, Tsujino H, Deushi M, Mizuta R, Yabu S, Obata A, Nakano H, Koshiro T, Ose T, Kitoh A (2012) A new global climate model of the Meteorological Research Institute: MRI-CGCM3 -model description and basic performance. J Meteorol Soc Jpn Ser II 90A:23–64
Yukimoto S, Kawai H, Koshiro T, Oshima N, Yoshida K, Urakawa S, Tsujino H, Deushi M, Tanaka T, Hosaka M, Yabu S, Yoshimura H, Shindo E, Mizuta R, Obata A, Adachi Y, Ishii M (2019) The Meteorological Research Institute Earth System Model Version 2.0, MRI-ESM2.0: description and basic evaluation of the physical component. J Meteorol Soc Jpn Ser II 97:931–965

Publisher's Note